Feedstock determines biochar-induced soil priming effects by stimulating the activity of specific microorganisms

Z . Y u[a],*, L . C h e n[b],*, S . P a n[a], Y . L i[a], Y . K u z y a k o v[c], J . X u[a], P . C . B r o o k e s[a] & Y . L u o[a]

[a]*Zhejiang Provincial Key Laboratory of Agricultural Resources and Environment, Institute of Soil and Water Resources and Environmental Science, Zhejiang University, Yuhangtang Road No.388 Hangzhou 310058, China,* [b]*State Key Laboratory of Soil and Sustainable Agriculture, Institute of Soil Science, Chinese Academy of Sciences, East Beijing Road No. 71 Nanjing 210008, China, and* [c]*Department of Soil Science of Temperate Ecosystems, University of Gottingen, Büsgenweg 2 37077 Gottingen, Germany*

Summary

Uncertainty remains over what properties of biochar and which groups of microorganisms are responsible for the direction and magnitude of observed biochar-induced priming effects (PE). We selected maize straw, grass, peanut shells and sugar cane as feedstocks to produce biochar at 300, 400 and 500°C by slow pyrolysis, and carried out an 80-day soil–biochar incubation experiment to investigate biochar-induced soil PE by adopting isotopic techniques. Irrespective of pyrolysis temperature, grass-derived biochar (Grass-B) induced the largest PE (348 to 1214 mg C kg^{-1} soil), whereas peanut shell-derived biochar (Peanut-B) induced the smallest (-135 to 261 mg C kg^{-1} soil) PE. The intensity of PE was largely determined by the feedstock and was closely related to the proportion of cellulose and lignin in it. The bacterial and fungal communities at days 8 and 40 were investigated by high-throughput sequencing of 16S rRNA and ITS genes. Biochar additions explained 54.0 and 52.9% of the total variation in bacterial and fungal community structure, respectively. The bacterial *Actinobacteria* and *Firmicutes* were dominant during the initial phase of the PE (at day 8), whereas the fungal *Sordariomycetes* and *Tremellomycetes* were abundant after the longer phase of incubation at day 40. A succession from bacterial community (used the available C fraction of biochar) to fungal community (used the recalcitrant C fraction of biochar and soil organic C) might occur during the PE, together with the alternation of apparent PE to real PE.

Highlights

- Feedstock type determines biochar-induced priming effects (PE).
- A succession from bacterial to fungal community occurred.
- *Actinobacteria* and *Firmicutes* used biochar available C during the early stage.
- *Sordariomycetes* and *Tremellomycetes* were associated with the later real PE.

Introduction

Biochar is the product of organic matter pyrolysed under oxygen-limited conditions, also termed pyrogenic organic matter (Maestrini *et al.*, 2015). Biochar application to soil as a long-term carbon (C) sink might help to mitigate climate change by sequestering C, so largely removing it from the C cycle (Sohi, 2012; Fang *et al.*, 2013; Luo *et al.*, 2016). The C sequestration potential of biochar relates to its slow microbial decomposition and chemical transformation (Kuzyakov *et al.*, 2009), based on evidence that biochar has been reported to remain for long periods in the

geological record and exist at soil depths where its residence time exceeds 1000 years (Sohi, 2012).

Biochar, however, is not totally biologically inert and contains labile and leachable C, in addition to strongly recalcitrant C (Lehmann *et al.*, 2011). Biochar can also change the rate of soil organic matter (SOM) mineralization (Luo *et al.*, 2011; Lu *et al.*, 2014; Whitman *et al.*, 2014). The short-term increases or decreases in SOM mineralization caused by the addition of organic substrates are known as priming effects (PEs) (Kuzyakov *et al.*, 2000). Previous studies have observed the different types of biochar-induced PEs: positive PEs (additional CO_2 release from SOM) (Wardle *et al.*, 2008; Luo *et al.*, 2011) and negative PEs (reduced CO_2 release from SOM) (Lu *et al.*, 2014). In some cases, an initial positive PE can transform into

Correspondence: Y. Luo. E-mail: luoyu@zju.edu.cn

*These authors contributed equally to this work.

a negative PE over time (Singh & Cowie, 2014; Whitman *et al.*, 2014).

Physicochemical characteristics of biochar depend on feedstock type and pyrolysis temperature (Singh *et al.*, 2010). For example, biochar often has higher aromatic density and pH with increasing pyrolysis temperature (Yuan *et al.*, 2011; Singh *et al.*, 2012), whereas feedstock type also affects biochar pH, for example wood biochar has a lower pH than maize straw biochar (Lehmann *et al.*, 2011). In general, woody plants have a large organic C content (48–54%) and small ash content (0.5–2%) and herbaceous plants have a slightly smaller organic C content (45–52%) and larger ash content (3–12%). By slow pyrolysis, 42–65% of organic C and nearly 100% of the mineral ash in the feedstock would be preserved (Moral *et al.*, 2005). Therefore, biochar derived from herbaceous plants probably has a large ash content, but small organic C content. The lignin and cellulose contents of feedstock also strongly affect the pore structure of biochar. A greater lignin content is responsible for a macroporous structure, whereas a greater cellulose content results in a microporous structure (Ioannidou & Zabaniotou, 2007).

A recent study showed that the intensity of biochar-induced PEs is mainly ascribed to feedstock type and pyrolysis temperature (Fang *et al.*, 2015). For example, biochar produced at low pyrolysis temperature usually induces short-term positive PEs (Luo *et al.*, 2011; Maestrini *et al.*, 2015). In general, wood and sugar bagasse-derived biochars (lignin-rich feedstocks) tend to induce negative PEs, whereas grass-derived biochars (cellulose-rich feedstocks) are more likely to cause positive PEs (Luo *et al.*, 2011; Maestrini *et al.*, 2015). However, the combined effects of different biochars produced by different feedstock types and pyrolysis temperatures on biochar-induced PEs have not yet been investigated under the same conditions.

Microorganisms are closely linked to the chemical composition of SOM and control the mineralization of SOM (Brookes *et al.*, 2017; Li *et al.*, 2017). Microorganisms compete with each other to acquire nutrients during a PE, specifically r- or K-strategists (copiotrophs or oligotrophs) control PEs by competing for nutrients under C-rich or C-limited conditions (Fontaine *et al.*, 2003). For example, PEs have recently been observed to be influenced by the addition of nitrogen (N), by modifying the decomposer community and balancing the r- and K-strategists, which was described as 'microbial N mining' and 'stoichiometric decomposition' theory (Fontaine *et al.*, 2003). Relations among biochar properties, PEs and microbial community structure are worth investigating. High-throughput sequencing technology has been widely used to determine soil microbial communities (Pezzolla *et al.*, 2015), and the link with its ecosystem functions can extend our understanding of the effects of soil microbes on PEs in biochar-amended soil.

Biochar-induced PEs have been largely determined by the different pyrolysis conditions and the feedstock types. Lignin and cellulose contents in feedstocks might have strong effects on biochar properties; therefore, we selected four types of feedstock based on their lignin and cellulose contents, and produced the biochars at different pyrolysis temperatures (300, 400 and 500°C). In this research, we performed an 80-day incubation experiment. Our objectives were to determine: (i) which factor (the pyrolysis temperature or feedstock type) dominates biochar-induced PEs and (ii) which microbial groups of bacteria and fungi are responsible for the observed PE during different incubation stages.

Materials and methods

Soil sampling and analysis

Soil (silt 21.7%, clay 28.1% and sand 50.2%, classified as a Utisol (USDA, 1998) was sampled from a long-term field experiment (120.23°N, 29.27°E) at the Dongyang Maize Institute of Zhejiang Academy of Agricultural Sciences in China. Maize (*Zea mays* L.) has been planted continuously for approximately 10 years. Soil samples were taken at intervals along the lines of a series of imaginary 'W's across the field, from the top 15 cm of the profile, and aggregated to one composite sample. After the visible plant debris and stones had been removed, soil samples were sieved (2-mm mesh) and homogenized, and a small portion of soil was used to measure basic physicochemical properties. Subsequently, soil moisture was adjusted to 40% of water holding capacity (WHC), and soils were pre-incubated at 25°C for 3 days to allow initial sampling and sieving effects to subside. Any N limitation was alleviated by the addition of NH_4NO_3 at 140 µg g^{-1} soil.

Soil pH was measured in a 1:2.5 soil solution (0.01 M CaCl$_2$). Total C and N contents were measured with a CNS-2000 dry combustion instrument (LECO, St. Joseph, MI, USA). Microbial biomass C (MBC) was analysed according to the fumigation–extraction method with a correction value of 0.45 (Vance *et al.*, 1987; Li *et al.*, 2013). The ^{13}C abundance ($\delta^{13}C$) was measured with an isotope ratio mass spectrometer (DELTA V plus IRMS) (Thermo Fisher Scientific, Bremen, Germany).

The initial δ^{13}C value of the soil was −23.54‰ Vienna-Pee Dee Belemnite (V-PDB). Soil (pH 4.4) contained 29.1 mg g^{-1} of organic C, 1.8 mg g^{-1} of total N, 96.0 µg g^{-1} of dissolved organic C and 73.0 µg g^{-1} of MBC.

Production and characterization of biochar

Grass, maize straw, sugarcane and peanut shells were chosen based on their different lignin and cellulose contents. A classic acid–detergent fibre with permanganate method was used to determine the lignin and cellulose contents in the feedstocks. The ratio of cellulose to lignin decreased in the order: grass > maize straw > sugarcane > peanut shells (Table 1). The four feedstocks were chopped into 2-cm pieces, firmly wrapped with aluminum foil and pyrolysed in a muffle furnace under oxygen-limited conditions. The rate of heating was 1°C minute^{-1} from 50 to 300, 400 and 500°C, followed by 30 minutes of continuous heating at the final temperature. The biochars produced were sieved to < 2 mm. We used 36 aluminum foils to produce 36 biochar samples (3 × 4 feedstocks used × 3 pyrolysis temperature levels). The biochars produced were sieved < 2 mm and the biochar properties were measured.

Table 1 Lignin and cellulose contents of feedstocks

	Maize straw / g kg^{-1}	Grass / g kg^{-1}	Peanut shells / g kg^{-1}	Sugarcane / g kg^{-1}
Lignin	142.4 ± 1.2	90.2 ± 2.1	287.6 ± 4.8	205.6 ± 2.8
Cellulose	312.3 ± 3.1	418.8 ± 4.7	159.3 ± 1.3	285.4 ± 3.3

Biochar ash content was measured as described by Yuan *et al.* (2011). The K$^+$ and Na$^+$ contents were determined by flame photometry, Ca^{2+} and Mg^{2+} contents by atomic absorption spectrometry, and cation exchange capacity (CEC) by a modified NH$_4$-acetate compulsory displacement method (Yuan *et al.*, 2011). Total C and N in biochars and feedstocks were measured by a CNS-2000 elemental analyser (LECO, St. Joseph, MI, USA). Dissolved organic C (DOC) was extracted at a biochar:water ratio of 1:10, and determined using a TOC auto-analyser (Shimadzu, Japan). The pH was measured at a 1:5 biochar:water ratio. The natural ^{13}C abundance of biochar was measured with an isotope ratio mass spectrometer (IRMS) (Thermo Fisher Scientific, Bremen, Germany).

Incubation experiment and sampling

An incubation experiment was carried out to investigate the priming effects of biochar on soil organic C and the mineralization of biochars with different pyrolysis temperatures (300, 400 and 500°C) and feedstock types (maize straw, grass, peanut shells and sugarcane). Twelve types of biochars were added separately to soil at 30 mg C g^{-1} soil. No biochar was added for the control. Each treatment included three replicates. Experimental units consisted of 40 g (dry weight basis) of moist pre-incubated soil treated with biochar and placed in 500-ml glass jars, which were incubated at 40% WHC and 25°C in the dark for 80 days. Maize-B, Grass-B, Peanut-B and Cane-B were the biochars derived from maize straw, grass, peanut shells and sugarcane, respectively. The pyrolysis temperatures of bicohar production were B300, B400 and B500.

An open vial containing 20 ml of 1.0 M NaOH was placed in each airtight jar to absorb CO_2 respired during each of the incubation periods. A beaker with 5 ml of deionized water was also placed at the bottom of each jar to prevent drying during incubation. Three extra jars containing NaOH and water only were incubated as blanks. At days 2, 4, 8, 20, 40 and 80 of incubation, the vials were replaced with another containing fresh NaOH, the jars were weighed and soil moisture was adjusted to retain 40% WHC. After the NaOH vials were removed from the jars, an excessive amount of 0.5 M BaCl$_2$ was added to them immediately to precipitate carbonate, and the remaining NaOH solution was titrated with 0.05 M HCl with an EasyPlus autotitrator (Mettler Toledo, Greifensee, Switzerland). The resulting BaCO$_3$ precipitates were filtered, carefully rinsed several times to pH 7 and freeze-dried for measurement of ^{13}C abundance. The natural ^{13}C abundance was measured using an isotope ratio mass spectrometer (IRMS) (Thermo Fisher Scientific, Bremen, Germany); more detail about the protocol is given in Luo *et al.* (2017). Soil from the jars was

sampled at days 8 and 40 of incubation, and stored at −80°C for microbial community analyses.

Partition and calculation of C mineralization

The mineralization of biochar was distinguished from soil organic C mineralization based on the changes in stable isotopic composition (δ^{13}C) over time.

The standard equation for determining δ^{13}C (‰) is derived from:

$$\delta^{13}C = \left[\left(R_{sample} / R_{VPDB} \right) - 1 \right] \times 1000, \qquad (1)$$

where R$_{sample}$ is the mass ratio of ^{13}C to ^{12}C and R$_{VPDB}$ is the international PDB limestone standard.

The differences between δ^{13}C values of soil and all biochars enable the separation of soil-derived and biochar-derived CO_2 using the mass balance equation:

$$F_{CO2-C,biochar} = \left(\delta^{13}_{sample}CO_2 - \delta^{13}_{soil}CO_2 \right) / \left(\delta^{13}_{biochar}CO_2 - \delta^{13}_{soil}CO_2 \right), \qquad (2)$$

where $F_{CO2-C,biochar}$ was the fraction of CO_2-C released from biochar in biochar-amended soil, $\delta^{13}_{sample} CO_2$ was the δ^{13}C value of the total CO_2-C released, $\delta^{13}_{soil} CO_2$ was the δ^{13}C value of CO_2-C released from soil without biochar, and $\delta^{13}_{biochar}CO_2$ was the δ^{13}C value of the initial biochar. The SOC mineralization ($F_{CO2-C,soil}$) was calculated from ($1 - F_{CO2-C,biochar}$). To evaluate the magnitude of the PE, we used the following equations to estimate the absolute amount of the PE and its relative magnitude:

$$\text{Priming effects (PE)} = F_{CO2-C,soil} \times CO_2 - C_{sample} - CO_2 - C_{soil} \qquad (3)$$

and

$$\text{Relative PE (\%)} = PE/CO_2 - C_{soil} \times 100, \qquad (4)$$

where CO_2-C$_{sample}$ and CO_2-C$_{soil}$ represented the total CO_2-C released from biochar-amended soil and non-amended soil, respectively, PE was the absolute value of soil organic carbon (SOC) primed by biochar and Relative PE was the percentage of the primed SOC relative to CO_2-C released from non-amended soil.

Extraction of DNA, amplicon library preparation and MiSeq sequencing

The DNA was extracted from 0.5 g of moist soil with a FastDNA Spin Kit for Soil (MP Biomedicals, Santa Ana, CA, USA) according to the manufacturer's protocol. The isolated DNA was dissolved in 50 μl of Tris-EDTA buffer, and the DNA quality and concentration were verified by electrophoresis on 1% agarose gels.

To produce the bacterial and fungal amplicon libraries for high-throughput sequencing, the bacterial 16S rRNA genes were amplified with the primers 515F (5′-GTGCCAGAMGCCGCGGTAA-3′) and 806R (5′-GGACTACHVGGGTWTCTAAT-3′) targeted on the V4 variable region, and the fungal rRNA genes were amplified

with the primer pair (5′-GCATCGATGAAGAACGCAGC-3′) and (5′-TCCTCCGCTTATTGATATGC-3′) targeted on the ITS3 region. To identify each sample, a unique 5-bp (base pair) barcode sequence was inserted into the 5′ end of the reverse primer. The PCR reaction mixes contained 0.5 µl (125 pmol) of each forward and reverse primer, 1 µl (50 ng) of genomic DNA, 23 µl of double distilled water and 25 µl of Premix Taq™ (Takara, Shiga, Japan). Thirty-five thermal cycles (30 s at 94°C, 30 s at 54°C and 45 s at 72°C) were carried out with a final extension for 10 minutes at 72°C.

The reaction products were cleaned and purified with a QIAquick PCR Purification Kit (Qiagen, Shenzhen, China), and quantified using an ND-1000 NanoDrop spectrophotometer (Thermo Scientific, Waltham, MA, USA). The amplicons were pooled at equimolar concentrations into a composite sample. The pooled sample was denatured with 0.1 M NaOH, diluted to 8 pM, and mixed with an equal volume of 8 pM Phix library. Finally, the prepared library mixture was mixed with read 1, read 2 and the index sequencing primers on a MiSeq Reagent Kit V2 (Illumina, San Diego, CA, USA), and dual index sequencing of the paired-end 250 base pair (bp) was run on an Illumina MiSeq instrument (Illumina). The sequences were submitted to the NCBI Sequence Read Archive (https://www.ncbi.nlm.nih.gov/sra/) with accession BioProject No PRJNA327718.

Data processing and analysis

Raw fastq files from bacterial and fungal sequencing were quality filtered and processed with the Quantitative Insights Into Microbial Ecology (QIIME) 1.9.0-dev pipeline (Caporaso *et al.*, 2010a). In brief, paired-end reads were assembled using the Fast Length Adjustment of SHort reads (FLASH) software. Barcode, linker primer, reverse primer and sequences with length less than 200 bp and ambiguous bases (long repeats of homopolymers > 8 bp) were discarded. The sequences were then grouped into operational taxonomic units (OTUs) by UPARSE (Edgar, 2013) based on 97% pairwise identity. Chimeric OTUs identified by UCHIME (v.4.2.40) (Edgar *et al.*, 2011) were removed. The most abundant sequence from each OTU was selected to represent that OTU. The representative OTU sequences were assigned to bacterial and fungal phylotypes with the RDP classifier (v.2.2) against a subset of the GREENGENES (release 2012. 03) and Silva 119 databases, respectively. The representative OTU sequences were aligned by PyNAST (Caporaso *et al.*, 2010b).

To avoid potential bias caused by sequencing depth, the subsets of 71 661 and 27 272 sequences were extracted randomly from each sample sequence for bacterial and fungal diversity analyses, respectively. Rarefaction analysis was based on 10 incremental 1000 sequences of random sub-sampling. To compare β-diversity between samples, non-metric multidimensional scaling analysis (NMDS) using the weighted UniFrac distances was calculated with the R package vegan. Permutational multivariate analysis of variance (PERMANOVA) was carried out with vegan's function adonis to measure the size of the effect of feedstock type, pyrolysis temperature, incubation time and their interactions on β-diversity

and its significance. PERMANOVA can partition distance matrices among sources of variation using a permutation test (Anderson, 2001). In addition, a hierarchical cluster analysis based on the Bray–Curtis dissimilarity matrix (Bray & Curtis, 1957) was performed using R's function hclust, and the output was then used to form a dendrogram.

Principle component analysis (PCA) was carried out with all biochar properties based on the correlation matrix method. Principal components (PCs) that explained more than 5% of the total variance were considered to be relevant (He *et al.*, 2009). Eigenvector values > 0.40 or < −0.4 were included in the interpretation of the PCs.

A two-way analysis of variance (ANOVA) was conducted to determine the effects of feedstock type, pyrolysis temperature and their interaction, both considered as fixed factors, on biochar properties and C mineralization, using SPSS 20.0 (SPSS Inc., Chicago, IL, USA). The assumptions of ANOVA were tested. Normality and homogeneity of variances were tested using the Shapiro–Wilk test and Levene's test, respectively, in SPSS. We used Fisher's least significant difference (LSD) to test for significant differences between individual means (Webster, 2007). Pearson's correlation analysis was also carried out to detect the relations between priming effects and mineralized carbon in biochar.

Results

Biochar properties and clusters of biochar samples

Peanut-B and Cane-B had larger total C and C/N, C/O and C/H ratios than Maize-B and Grass-B, indicating that the former contained fewer polar functional groups and more aromatic structures. Maize-B and Grass-B had larger ash and DOC contents than Peanut-B and Cane-B. With the increase in pyrolysis temperature, DOC content in Maize-B and Grass-B decreased markedly (Table 2).

Principle component analysis (PCA) was carried out to separate the effects of feedstock type and pyrolysis temperature on biochar properties. Principle component 1 (PC1) explained most of variation in the biochar properties (52.2%), which the plot of the eigenvectors of biochar samples (Figure 1b and Table S1, Supporting Information) shows is closely related to feedstock types, especially to lignin and cellulose contents. For example, the C/N ratio is strongly negatively related to PC1 and ash content is strongly positively related to it. Principle component 2 (PC2) explained 26.9% of variation in biochar properties; pH is strongly positively related to it and CEC is strongly negatively related. Figure 1(a) shows the PC scores plotted in the plane of the first two principal components. They show that PC1 relates to the different feedstocks, with grass and maize on the positive side of PC1 and peanut and cane on the negative side. The temperature of pyrolysis for grass shows a wide distribution along PC1, with low temperature pyrolysis on the negative side and high temperature pyrolysis on the positive side. Maize is less strongly distributed along PC2, but it follows a similar pattern to grass. Cane, however, shows no relation with PC2 and that of peanut is modest compared with grass and maize (Figure 1b).

Table 2 Two-way analysis of variance (ANOVA) of the effects of feedstock type (F), pyrolysis temperature (T) and their interaction (F•T) on biochar properties

		Temp 300	Temp 400	Temp 500	Mean	Source of variation	d.f.	F	P	SE	LSD
Total C / %	Maize	48.7	50.3	53.4	50.8	Feedstock (F)	3	36.7	<0.001	2.00	9.00
	Grass	40.7	45.9	52.9	46.5	Temperature (T)	2	12.1	<0.001	1.73	10.54
	Peanut	54.5	70.2	74.6	66.4	F•T	6	1.1	NS	3.46	
	Sugarcane	65.9	72.1	76.9	71.7	Error	24				
	Mean	52.4	59.6	64.4							
C/N	Maize	29.2	30.3	31.1	30.2	Feedstock (F)	3	763.2	<0.001	1.01	4.56
	Grass	19.3	20.2	20.6	20.0	Temperature (T)	2	0.4	NS	0.88	
	Peanut	67.2	68.1	68.7	68.0	F•T	6	0.2	NS	1.76	
	Sugarcane	78.2	76.0	77.7	77.3	Error	24				
	Mean	48.5	48.6	49.5							
C/H	Maize	13.6	14.7	19.7	16.0	Feedstock (F)	3	118.9	<0.001	0.61	2.75
	Grass	11.0	15.1	23.3	16.5	Temperature (T)	2	36.5	<0.001	0.53	3.22
	Peanut	20.3	22.5	26.1	22.9	F•T	6	5.5	0.001	1.06	3.67
	Sugarcane	30.7	29.0	31.0	30.2	Error	24				
	Mean	18.9	20.3	25.0							
C/O	Maize	2.5	2.6	2.6	2.6	Feedstock (F)	3	11.8	<0.001	0.33	1.48
	Grass	2.2	2.4	2.7	2.4	Temperature (T)	2	5.5	0.011	0.29	1.73
	Peanut	2.6	4.4	5.3	4.1	F•T	6	1.2	NS	0.57	
	Sugarcane	3.6	4.8	5.7	4.7	Error	24				
	Mean	2.7	3.5	4.1							
Ash / %	Maize	18.8	20.2	23.6	20.9	Feedstock (F)	3	2244.7	<0.001	0.25	1.11
	Grass	23.8	32.4	37.7	31.3	Temperature (T)	2	120.1	<0.001	0.21	1.30
	Peanut	7.5	7.4	7.3	7.4	F•T	6	61.0	<0.001	0.43	1.48
	Sugarcane	7.0	6.9	7.2	7.0	Error	24				
	Mean	14.3	16.7	19.0							
DOC / mg kg^{-1}	Maize	837.0	600.0	245.0	560.7	Feedstock (F)	3	14 457.7	<0.001	2.84	12.80
	Grass	1806.0	458.0	117.0	793.7	Temperature (T)	2	14 361.0	<0.001	2.46	14.99
	Peanut	81.0	81.0	70.0	77.3	F•T	6	7394.6	<0.001	4.93	17.04
	Sugarcane	150.0	143.3	136.0	143.1	Error	24				
	Mean	718.5	320.6	142.0							
pH	Maize	9.6	10.1	10.6	10.1	Feedstock (F)	3	3080.5	<0.001	0.01	0.03
	Grass	7.9	10.2	10.4	9.5	Temperature (T)	2	9874.6	<0.001	0.01	0.03
	Peanut	10.1	10.2	10.3	10.2	F•T	6	3986.6	<0.001	0.01	0.03
	Sugarcane	9.7	9.7	9.8	9.8	Error	24				
	Mean	9.3	10.0	10.3							
δ^{13}C	Maize	−14.4	−14.3	−14.2	−14.3	Feedstock (F)	3	10 321.9	<0.001	0.08	0.36
	Grass	−28.5	−28.6	−28.2	−28.4	Temperature (T)	2	3.1	NS	0.07	
	Peanut	−27.9	−28.0	−28.0	−28.0	F•T	6	0.8	NS	0.14	
	Sugarcane	−13.7	−14.0	−13.5	−13.7	Error	24				
	Mean	−21.1	−21.2	−21.0							
CEC / cmol kg^{-1}	Maize	67.4	116.2	145.9	109.8	Feedstock (F)	3	6419.1	<0.001	0.31	1.39
	Grass	80.9	119.7	167.0	122.5	Temperature (T)	2	8646.9	<0.001	0.27	1.62
	Peanut	106.3	114.4	187.0	135.9	F•T	6	4157.0	<0.001	0.53	1.85
	Sugarcane	97.9	86.2	50.4	78.2	Error	24				
	Mean	88.1	109.1	137.6							
Total K / mg g^{-1}	Maize	4.8	8.6	10.9	8.1	Feedstock (F)	3	68 214.0	<0.001	0.06	0.26
	Grass	26.2	38.5	47.4	37.4	Temperature (T)	2	4879.4	<0.001	0.05	0.31
	Peanut	4.9	5.1	5.1	5.0	F•T	6	2401.2	<0.001	0.10	0.35
	Sugarcane	8.0	7.9	8.6	8.2	Error	24				
	Mean	11.0	15.0	18.0							

Total C, total carbon; C/N, carbon/nitrogen ratio; C/H, carbon/hydrogen ratio; C/O, carbon/oxygen ratio; DOC, dissolved organic carbon; CEC, cation exchange capacity; Total K, total potassium; Temp300, pyrolysis at 300°C; Temp400, pyrolysis at 400°C; Temp500, pyrolysis at 500°C; d.f., degrees of freedom; SE, standard error of means of feedstock type, pyrolysis temperature and their interaction; LSD, least significant difference for the effects that are significant; NS, not significant.
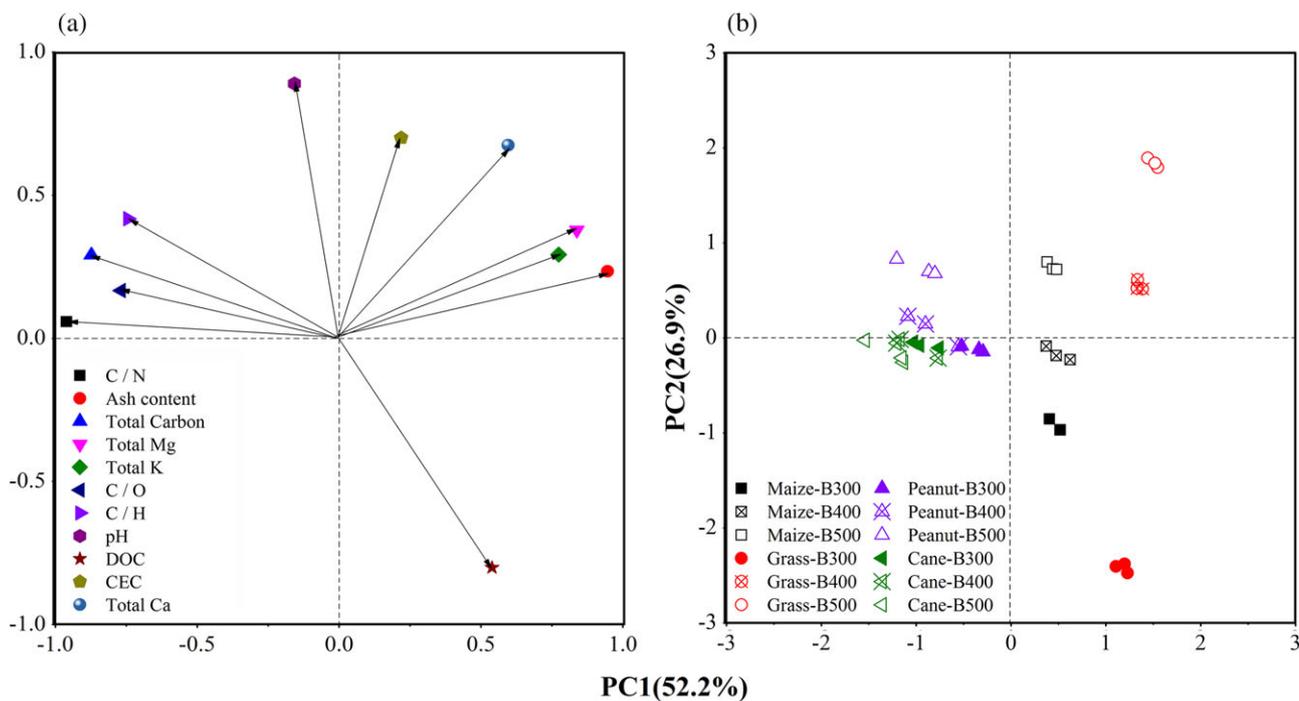
Figure 1 Principal component analysis (PCA) of biochar samples: (a) plot of the eigenvectors and (b) plot of the PC scores in the plane of principal components 1 and 2.

Feedstocks with large lignin contents (peanut shells and cane) produced biochars with lower polar groups (i.e. larger C/N and C/O ratios) and larger total carbon. Feedstocks with large cellulose contents (maize and grass), produced biochars rich in ash content, total K^+ and Mg^{2+}. Biochar CEC and pH were closely related to pyrolysis temperature: higher temperatures led to larger CEC and higher pH values. Dissolved organic carbon (DOC) and C/H depended on both cellulose and lignin contents in the feedstocks and pyrolysis temperatures (Figure 1a and Table S1). In general, biochar derived from feedstocks with large cellulose contents and at low temperatures had large labile C contents and low aromatic densities. Cellulose and lignin contents in feedstocks have close relations with total carbon, C/O ratio, C/N ratio and ash content in biochar. Feedstock type was the primary factor for the differentiation in biochar properties, and pyrolysis temperature affected the biochar properties based on feedstock type.

Cumulative mineralization of biochar and induced PE

On a cumulative basis, total CO_2 emission from soil samples amended with biochar was significantly larger than that from non-amended soil samples. Total CO_2 emission from soil amended with biochars with large cellulose contents in their feedstocks (i.e. Maize-B and Grass-B) was significantly larger than that from biochars with large lignin contents in their feedstocks (i.e. Peanut-B and Cane-B), independently of pyrolysis temperature (Table 3). The largest CO_2 emission was from soil amended with Grass-B300 (3148.6 mg C kg^{-1} soil), whereas the soil amended with Peanut-B

had the smallest CO_2 emission (936.7 to 1230.4 mg C kg^{-1} soil), regardless of pyrolysis temperature. Pyrolysis temperature changed CO_2 emission significantly from soil amended with only Maize-B and Grass-B, indicating that the effects of pyrolysis temperature depend on feedstock types (Figure 2 and Table 3).

The PE was positive in all soil samples with biochar, except for Peanut-B300 (-135.1 mg C kg^{-1} soil). Mineralized SOM at 80 days of incubation ranged from 1.97 to 6.63% of initial SOC content, whereas in soil without biochar, mineralized C at 80 days was 2.44% (Table 3). The most intensive mineralization of SOM occurred during the first 4 days of incubation, followed by a gradual decrease (except for the soil amended with Cane-B) (Figure S1). The biochar derived from the feedstock with the largest cellulose content, Grass-B, induced the largest PE, which decreased considerably as the pyrolysis temperature of the biochar increased (1214.5 to 348.3 mg C kg^{-1} soil). Peanut-B was derived from the feedstock with the largest lignin content, which induced the smallest PE (-135.1 to 261.4 mg C kg^{-1} soil) independently of temperature (Table 3). This is similar to the total CO_2 emission from samples with Peanut-B addition, suggesting that the effect of pyrolysis temperature on PEs depends largely on the type of feedstock during slow pyrolysis.

Biochar mineralization in soil with biochar addition ranged from 5.1 to 40.9‰ during the 80-day incubation. The ratio of mineralized SOM to mineralized biochar was smaller in soil with Maize-B and Grass-B (36.4–66.3‰ of SOC) than in soil with Peanut-B and Cane-B (19.7–46.8‰ of SOC). The amounts of biochar mineralization were less in soil with Peanut-B and Cane-B (5.1–12.1‰

Table 3 Two-way analysis of variance (ANOVA) of the effects of feedstock type (F), pyrolysis temperature (T) and their interaction (F•T) on cumulative mineralization of SOM, biochar and induced priming effect

		Temp300	Temp400	Temp500	Mean	Source of variation	d.f.	F	P	SE	LSD
Total CO_2-C at 80 days / mg C kg^{-1} dry soil	Maize	2114.0	1982.2	1533.5	1876.6	Feedstock (F)	3	343.7	<0.001	28.57	128.55
	Grass	3148.6	2196.2	1535.8	2293.5	Temperature (T)	2	68.2	<0.001	24.74	150.54
	Peanut	936.7	1044.9	1230.4	1070.7	F•T	6	84.9	<0.001	49.48	171.22
	Sugarcane	1294.0	1482.2	1559.2	1445.1	Error	24				
	Mean	1873.3	1676.4	1464.7							
Mineralized C at 80 days / ‰ initial SOC	Maize	48.0	45.6	37.5	43.7	Feedstock (F)	3	912.6	<0.001	0.34	1.52
	Grass	66.3	49.9	36.4	50.9	Temperature (T)	2	69.0	<0.001	0.29	1.78
	Peanut	19.7	27.2	33.4	26.8	F•T	6	284.0	<0.001	0.59	2.02
	Sugarcane	39.3	43.4	46.8	43.2	Error	24				
	Mean	43.4	41.5	38.5							
Mineralized C at 80 days / ‰ biochar C	Maize	24.0	22.0	14.8	20.3	Feedstock (F)	3	808.2	<0.001	0.34	1.52
	Grass	40.9	25.0	16.1	27.3	Temperature (T)	2	232.6	<0.001	0.29	1.79
	Peanut	12.1	8.5	8.7	9.8	F•T	6	102.6	<0.001	0.59	2.03
	Sugarcane	5.1	7.2	6.7	6.3	Error	24				
	Mean	20.5	15.7	11.6							
Primed C at 80 days / mg C kg^{-1} dry soil	Maize	685.6	613.6	381.0	560.1	Feedstock (F)	3	985.2	<0.001	9.42	42.39
	Grass	1214.5	740.8	348.3	767.9	Temperature (T)	2	74.5	<0.001	8.16	49.64
	Peanut	−135.1	81.0	261.4	69.1	F•T	6	306.6	<0.001	16.32	56.46
	Sugarcane	433.5	552.1	650.2	545.2	Error	24				
	Mean	549.6	496.9	410.2							
Relative priming effect / %	Maize	97.2	87.2	54.0	79.5	Feedstock (F)	3	227.8	<0.001	2.78	12.5
	Grass	172.2	105.2	49.6	109.0	Temperature (T)	2	17.1	<0.001	2.41	14.64
	Peanut	−19.0	11.5	37.1	9.9	F•T	6	70.7	<0.001	4.81	16.65
	Sugarcane	61.6	78.3	92.3	77.4	Error	24				
	Mean	78.0	70.5	58.3							

Temp300, pyrolysis at 300°C; Temp400, pyrolysis at 400°C; Temp500, pyrolysis at 500°C; d.f., degrees of freedom; SE, standard error of means of feedstock type, pyrolysis temperature and their interaction; LSD, least significant difference for the effects that are significant.

of biochar-C) than with Maize-B and Grass-B (14.8–40.9‰ of biochar-C) (Table 3). Cumulative biochar mineralization was positively related to cumulative PEs in samples with Maize-B and Grass-B ($r = 0.96$, $P < 0.01$) (Figure 3a), whereas in Peanut-B and Cane-B samples the relations were negative ($r = -0.65$, $P < 0.01$) (Figure 3b), indicating that interactions between biochar and SOM mineralization might be different among types of feedstock.

Bacterial and fungal community composition and diversity

In soil with or without biochar, major bacterial phyla with average relative abundances of more than 5% were *Actinobacteria*, *Proteobacteria*, *Chloroflexi*, *Firmicutes* and *Acidobacteria*. The *Actinobacteria* and *Proteobacteria* dominated the bacterial community, accounting for 38.4 and 22.9% on average of the bacterial sequences, respectively. The relative abundance of *Actinobacteria* increased, whereas *Proteobacteria* decreased from day 8 to day 40. *Firmicutes* were more abundant in Maize-B300 and Grass-B300 than Maize-B500 and Grass-B500 on both sampling days. *Chloroflexi* showed the reverse pattern and they were abundant in Maize-B500 and Grass-B500 (Figure 4). The phyla *Ascomycota*, *Basidiomycota* and *Zygomycota* dominated the fungal community. *Ascomycota* was the predominant fungal population during the

incubation, comprising on average 45.1% of the fungal sequences. The population of *Agaricomycetes* was larger in samples with Peanut-B and Cane-B, but *Sordariomycetes* were more abundant in soil with Maize-B and Grass-B, especially for the lower temperature pyrolysis treatments (Figure 4).

The bacterial community showed greater α-diversity in biochar-amended soil at a high pyrolysis temperature than at low temperature on day 8, which was more pronounced in soil with Maize-B and Grass-B (Table S2, Supporting Information). We observed that the bacterial communities in the soils amended with Peanut-B and Cane-B were more clustered at days 8 and 40 than those amended with Grass-B and Maize-B (Figure 5a,c). In contrast, the fungal community showed little convergence to groups between different biochar treatments (Figure 5b,d). We used permutational multivariate analysis of variance (PERMANOVA) to quantify the effect of size and significance of groups based on weighted UniFrac distances (Table 4). Overall, the present data explained more than half of the variation in microbial community (54.0 and 52.9% for bacterial and fungal communities, respectively). Incubation time was the primary source of variation in the bacterial community and explained 25.9% ($P < 0.01$). In contrast, feedstock type was the principal source of variation in the fungal community and explained 18.8% ($P < 0.01$). Pyrolysis temperature
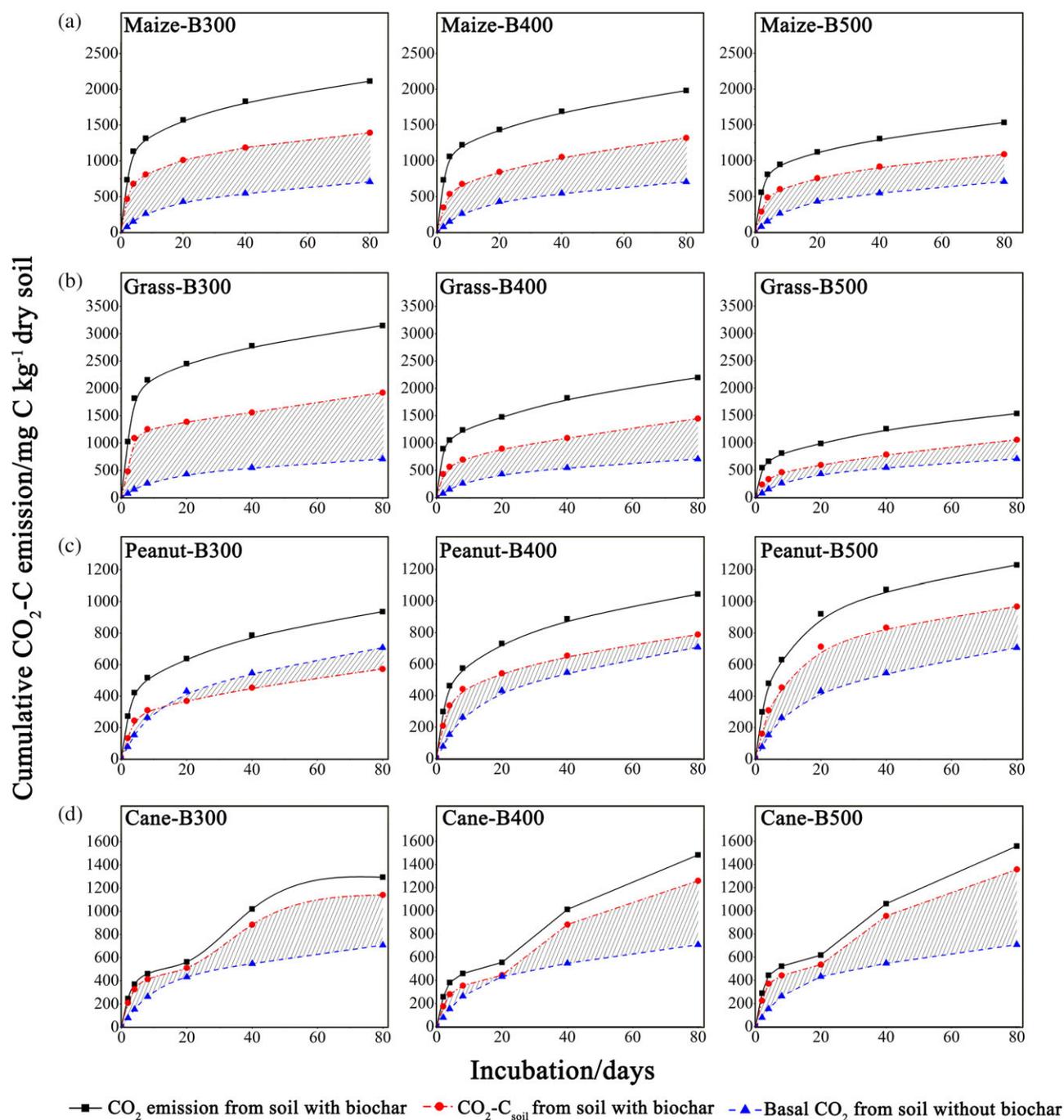
Figure 2 Cumulative CO_2 emission from soil amended with four feedstocks: row (a) maize, (b) grass, (c) peanut and (d) cane. Each feedstock was pyrolysed at 300, 400 or 500°C. Grass, maize, peanut and cane were feedstocks of biochar. B-300, B-400 and B-500 represented pyrolysis temperatures. The marked area represents priming effects (PEs).

accounted for 8.2 and 7.7% of variation in the bacterial and fungal communities, respectively (Table 4). Feedstock type explained a significant ($P \leq 0.01$) proportion of the variation: 39.3 and 31.4% for bacterial and fungal communities, respectively. Pyrolysis temperature accounted for 12.5 and 11.4% of bacterial and fungal community variation, respectively (Table 4).

Discussion

Biochar properties determined PE

We conducted a biochar-induced PE experiment with two groups of feedstock types based on lignin and cellulose content in feedstocks. Grass (rich in cellulose) derived biochar (Grass-B) induced the
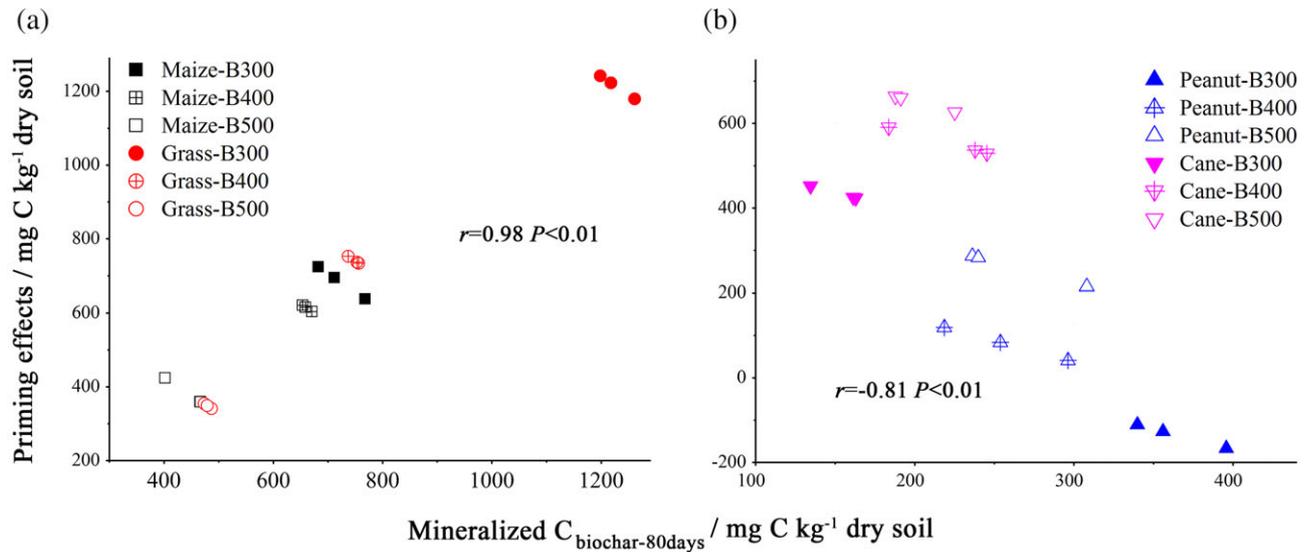
Figure 3 Relations between the intensity of priming effects (PEs) and mineralized $C_{biochar}$ after 80 days ($C_{biochar\text{-}80\,days}$) in soil with added biochar produced from (a) maize straw and grass and (b) peanut shells and cane. For each feedstock type, data from biochar pyrolysed at 300, 400 and 500°C were used.
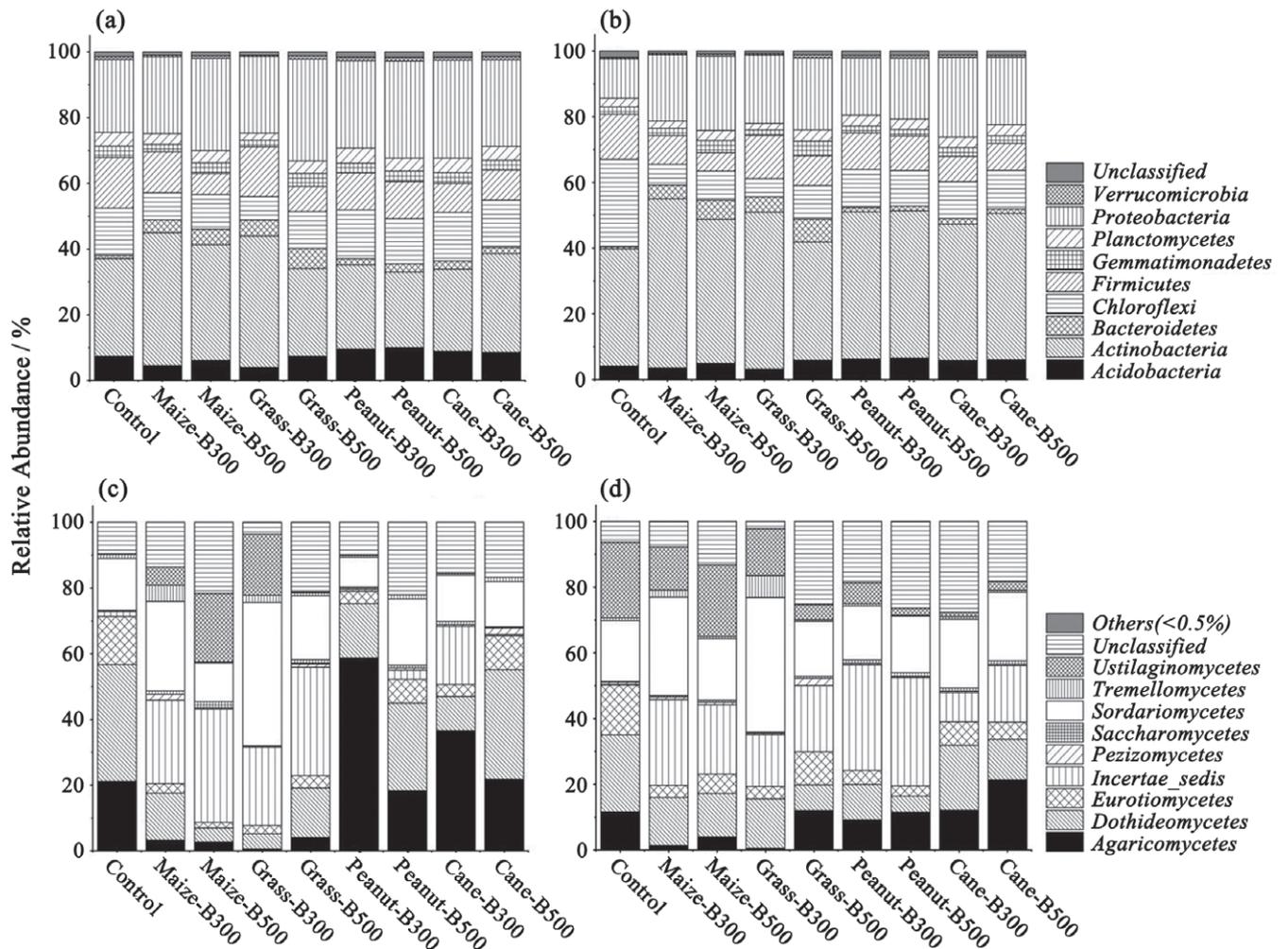

Figure 4 Relative abundance of bacterial phyla at (a) day 8 and (b) day 40, and fungal classes at (c) day 8 and (d) day 40 after incubation in soil with and without the addition of biochars derived from four feedstocks pyrolysed at 300 and 500°C.
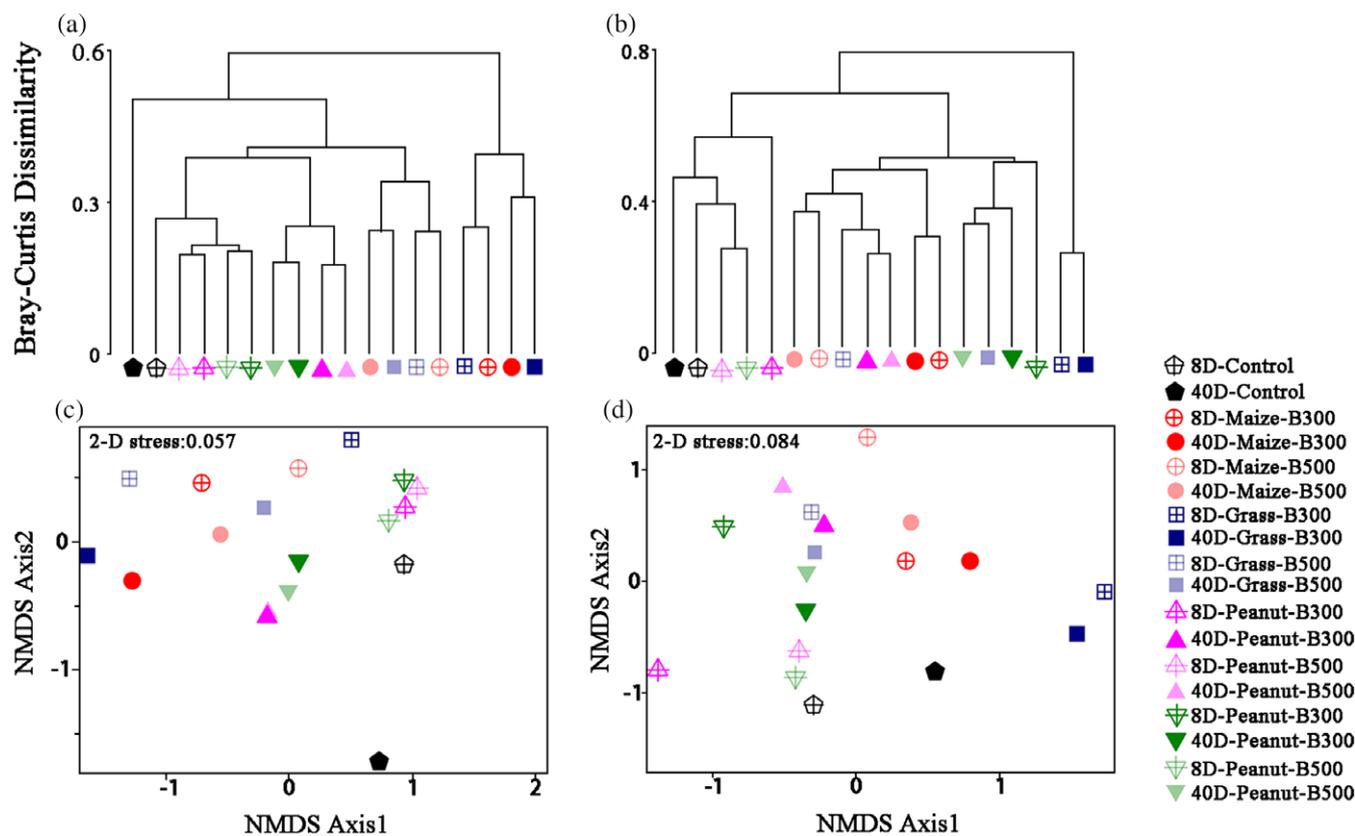
Figure 5 Dendrograms derived from the Bray–Curtis dissimilarity matrix between samples by the unweighted pair-group method with arithmetic means (UPGMA) for (a) the bacterial and (b) fungal communities. The plots of non-metric multidimensional scaling analysis (NMDS) based on the weighted UniFrac distances of (c) bacterial and (d) fungal communities, respectively, plotted in the plane of the first two axes. The stress values indicate goodness of fit of NMDS. In general, results of NMDS with the stress < 0.2 are acceptable.

largest PE, which declined considerably as pyrolysis temperature increased (Figure 2), whereas Peanut-B, which had the largest lignin content in the feedstock, induced the smallest PE (Figure 2). Our results support previous research (Luo *et al.*, 2011; Singh *et al.*, 2012), which demonstrated that SOM mineralization was greater in soil with inputs of grass-derived biochars than wood-derived biochars. A meta-analysis on approximately 650 data points from 18 studies showed that grass-derived biochar induced a larger positive PE than biochars derived from other feedstocks (Maestrini *et al.*, 2015); this is consistent with our results. To investigate which properties of biochar determine PE intensity, we correlated cumulative PE with measured biochar properties. The magnitude of cumulative PE was positively correlated with ash content ($r = 0.60$, $P < 0.01$) and DOC ($r = 0.97$, $P < 0.01$), but negatively correlated with the C/N ($r = -0.79$, $P < 0.01$) and C/H ($r = -0.77$, $P < 0.01$) ratios and pH ($r = -0.76$, $P < 0.01$), especially during the first 20 days of incubation (Table S3, Supporting Information).

We observed the strongest positive correlation between DOC and PE following 8 days of incubation ($r = 0.97$, $P < 0.01$). Likewise, Maestrini *et al.* (2014) observed a strong positive PE during the first 18 days of incubation with the addition of grass biochar, which they attributed to labile carbon-caused co-metabolism. Luo *et al.* (2011)

found a strong correlation between available C within biochar and positive PE, and considered that increased available C causes microbial activation that enhances SOM mineralization.

Other soil properties such as texture, C/N, pH and soil organic matter content could also be important factors controlling biochar-induced PEs (Maestrini *et al.* 2015). The larger C/N ratio of Peanut-B was negatively correlated with the magnitude of PE, which can be attributed to the intensive aromatic structure and small nitrogen content in this lignin-rich feedstock (i.e. peanut shells) (Hilscher *et al.*, 2009). The pH value of biochar was negatively related to biochar-induced PE in this research (Table S3). However, Maestrini *et al.* (2015) found no relation between the magnitude of PE and pH values of biochar based on a meta-analysis. A large ash content in biochar might contribute essential elements such as Mg^{2+} and K^+ (Deenik *et al.*, 2011) and indirectly enhance the PE through its positive effect on pH. However, ash did not appear to be as strongly associated with PEs as some other properties such as DOC, C/N, C/H and pH in this study (Table S3).

Biochar mineralization and its induced soil PE

Positive correlations between the mineralization of biochar (Maize-B and Grass-B) and the corresponding PE supported

Table 4 Effects of feedstock and temperature on bacterial and fungal community structure tested by PERMANOVA based on the weighted UniFrac distance matrices

	Mean squares	Variation explained / %	F	P
Bacterial community				
Feedstock	0.107	39.3	3.021	0.010
Temperature	0.102	12.5	2.898	0.053
Feedstock and temperature	0.037	13.6	1.053	0.430
Residual	0.035	34.6		
Fungal community				
Feedstock	0.215	31.4	2.815	0.007
Temperature	0.235	11.4	3.066	0.019
Feedstock and temperature	0.189	27.5	2.471	0.020
Residual	0.077	29.7		

The significance (*P*) was examined by *F*-tests based on sequential sums of squares from 999 permutations of operational taxonomic units (OTU) sequences.

the mechanism of co-metabolism (Figure 3a). Our previous studies using scanning electron microscopy (SEM) images and biomass ^{13}C analysis provided direct evidence of microbial colonization

and utilization of biochar C, indicating the potential co-metabolism of biochar with SOM mineralization (Luo *et al.,* 2011, 2013).

Negative correlations between biochar mineralization and PE were also observed in soils with Peanut-B and Cane-B (Figure 3b), indicating that interactions between biochar and SOM were more complicated than previously expected and largely dependent on the feedstocks. Tian *et al.* (2016) observed that microorganisms would start to use N from the SOM to compensate for large C:N ratios after biochar application. However, we added N to alleviate its limitation in soil so that the 'Mining theory' could be largely excluded. The relatively lignin-enriched Peanut-B and Cane-B were more recalcitrant, thus microbial organisms might preferentially use labile C released from SOM rather than the biochar (Fontaine *et al.*, 2003). This could be a reason for the negative correlation between biochar and SOM mineralization, especially under available C-limited conditions because lignin-rich feedstock-derived biochar was added to soil.

Pyrolysis temperature and feedstock adjusted microbial community

Higher pyrolysis temperatures might have more positive effects on richness and diversity of the bacterial community than low pyrolysis

Table 5 Correlations between cumulative priming effects (PEs) and the abundance of microbial taxa

	Cumulative PE at 8 days		Cumulative PE at 40 days	
Microbial population	Pearson correlation coefficient (*n* = 8)	*P* (two-tailed)	Pearson correlation coefficient (*n* = 8)	*P* (two-tailed)
Bacterial phylum				
Acidobacteria	−0.516	0.190	−0.689	0.059
Actinobacteria	***0.839***	0.009	0.545	0.162
Bacteroidetes	0.549	0.159	0.367	0.371
Chloroflexi	−0.528	0.178	**−0.760**	0.029
Firmicutes	**0.739**	0.036	0.345	0.402
Gemmatimonadetes	−0.212	0.614	−0.260	0.535
Planctomycetes	−0.438	0.278	−0.671	0.068
Proteobacteria	0.126	0.765	0.451	0.261
Fungal class				
Dothideomycetes	−0.520	0.187	0.633	0.092
Eurotiomycetes	−0.462	0.249	−0.134	0.752
Ascomycota, Incertae sedis	−0.390	0.340	0.269	0.519
Leotiomycetes	−0.294	0.479	−0.148	0.726
Pezizomycetes	−0.126	0.767	−0.093	0.826
Saccharomycetes	−0.165	0.696	***−0.853***	0.007
Sordariomycetes	0.678	0.065	***0.853***	0.007
Agaricomycetes	−0.597	0.118	−0.578	0.134
Pucciniomycetes	−0.173	0.682	0.107	0.800
Tremellomycetes	0.409	0.315	**0.832**	0.010
Ustilaginomycetes	**0.796**	0.018	0.529	0.178
Chytridiomycetes	−0.254	0.544	−0.483	0.225
Unclassified class	−0.561	0.148	−0.631	0.093
Zygomycota, Incertae sedis	0.206	0.625	−0.220	0.601

The values in bold show significant correlations at the 0.05 level, and the values in bold and italic at the 0.01 level.
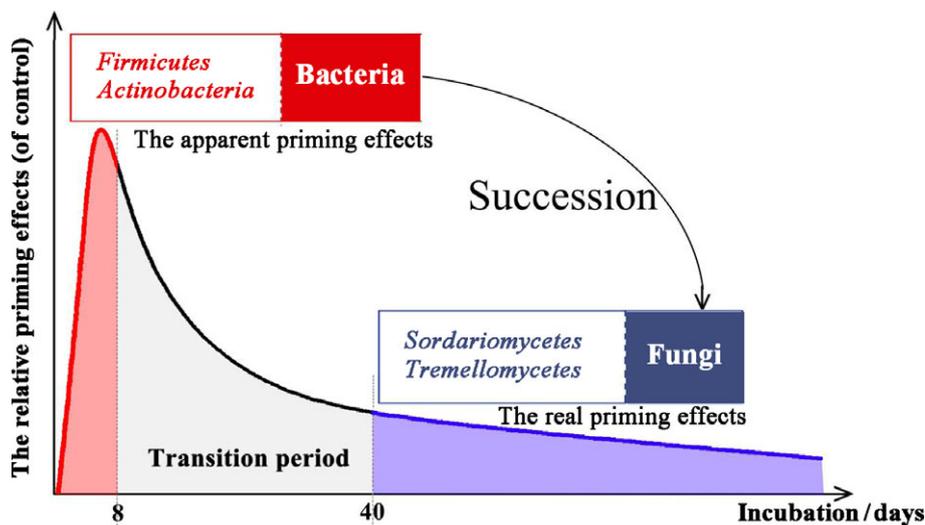
Figure 6 Graphical speculation of a microbial community succession from the dominance of bacteria to fungi, together with the alternation of priming effects (PEs) over incubation time.

temperature (Table S2). Likewise, Hale *et al.* (2015) reported that the density of the bacterial population increased with wood biochar produced at 600°C as an inoculum carrier, compared with biochar produced at 300°C. However, Dai *et al.* (2017) reported biochar produced at 300°C had a larger total microbial activity and more diverse bacterial communities than biochar produced at 700°C. Feedstock type explained more of the variation in the microbial community for both bacteria (39.3%) and fungi (31.4%) than temperature (Table 4). This was probably because of the difference in DOC, ash content, C/N and C/H, which were closely associated with feedstock types. For example, the C/N ratio of biochar, as reported by Rousk *et al.* (2013), was attributed to the difference in the fungi:bacteria ratio of biochar-amended soil.

Apparent and real PE together with a shift in microbial community

Previous studies have identified certain species of decomposers in the bacterial community adapted to different substrates. *Actinobacteria*, *Gemmatimonadetes*, *Bacteroidetes* and *Firmicutes* were identified as biochar C decomposers (Khodadad *et al.*, 2011; Watzinger *et al.*, 2014; Pezzolla *et al.*, 2015), which partly agreed with our results that Ac*tinobacteria* (G$^+$) and *Firmicutes* (G$^+$), affiliated to bacteria, had positive significant correlations ($r > 0.7$) with the cumulative PE at day 8 (*Firmicutes* and *Actinobacteria*) (Table 5). In other studies, *Actinobacteria* were also identified as an SOM-degrading population and possibly involved in either or both the redistribution of previously consumed C or in the degradation of more recalcitrant compounds (Khodadad *et al.*, 2011).

The abundance of *Sordariomycetes* and *Tremellomycetes*, which are affiliated to fungi, was positively correlated with the cumulative PE at day 40 (Table 5). Long-term PE can probably be attributed to degradation of the relatively recalcitrant SOM pool. Changes in long-term priming effects might be associated with specific fungi or the activities of other species that can mineralize recalcitrant C. Other research has reported that Gram-negative

bacteria dominated immediately following biochar addition, with a shift to Gram-positive bacteria with time (Mitchell *et al.*, 2015). In our research, the initial CO_2 flush (i.e. in the first 8 days) of SOM mineralization (Figure S1) was considered to be almost all derived from the fast turnover of microorganisms, which was termed 'Apparent Priming effects' (Blagodatskaya & Kuzyakov, 2008). The fast turnover of microorganisms might be attributed to their adaption to the addition of biochar and metabolism of the degradable fraction of biochar (Luo *et al.*, 2011). After labile C from biochar disappeared, degradation of the recalcitrant SOM might occur, but it is definitely not the major source of the initial CO_2 flush, especially after the early stage during incubation. At day 40, the rapid emission of CO_2 from the turnover of microorganisms was replaced by a slower emission of CO_2 from the degradation of SOM, which was termed the 'Real Priming effects' (Blagodatskaya & Kuzyakov, 2008).

Together with the shifts in mineralization of biochar C to SOM pools during PEs, a microbial community succession from the dominance of bacteria to fungi or to microbes that can degrade recalcitrant C might also occur during the PE (Figure 6). To demonstrate this hypothesis, DNA−SIP coupled with high-throughput sequencing are promising tools to make further progress in understanding the biochar-induced PE and responsible microbial groups.

Conclusions

At all pyrolysis temperatures Grass-Biochar induced the largest priming effects, whereas Peanut-Biochar induced the smallest, including the only negative PE, indicating that feedstock is the major factor related to PEs induced by various biochars. Different proportions of cellulose and lignin contents might be one of the reasons; they are associated with properties of biochar such as DOC, ash and C/N ratio. Thus, biochar derived from feedstock with a large lignin content tends to increase the C sequestration potential rather than other types of feedstock. There was an inverse interaction between SOM and biochar mineralization. Co-metabolism

could be explained by the positive correlation between SOM and biochar mineralization, whereas a negative correlation might be attributed to preferentially used labile C from SOM. The initial phase (day 8) of the PE (i.e. the fast response after biochar addition) probably resulted from the stimulation of endogenous bacterial metabolism, for which *Actinobacteria* (G$^+$) and *Firmicutes* (G$^+$) were plausibly responsible. Fungal activity, especially *Sordariomycetes* and *Tremellomycetes*, was related to the second and longer phase (day 40) of the PE (most probably the real PE). Considering the shift from C in mineralizing biochar to SOM pools, a microbial community succession from the dominance of bacteria to fungi (or microbes that degrade recalcitrant C) might occur during the biochar-induced PE.

Supporting Information

The following supporting information is available in the online version of this article:

Table S1. Eigenvalues and eigenvectors of the leading principal components based on biochar properties.

Table S2. The bacterial and fungal alpha diversity across all biochar–soil combinations at days 8 and 40 of incubation.

Table S3. Correlation analysis between magnitude of priming effects (PEs) and properties of biochar.

Figure S1. Relative priming effects (PEs) (compared to basal respiration) induced by 12 biochar types derived from four feedstock types: (a) maize straw, (b) grass, (c) peanut shells and (d) sugar cane, pyrolysed at 300, 400 and 500°C.

Acknowledgements

References

Anderson, M.J. 2001. A new method for non-parametric multivariate analysis of variance. *Austral Ecology*, **26**, 32–46.

Blagodatskaya, E. & Kuzyakov, Y. 2008. Mechanisms of real and apparent priming effects and their dependence on soil microbial biomass and community structure: critical review. *Biology and Fertility of Soils*, **45**, 115–131.

Bray, J.R. & Curtis, J.T. 1957. An ordination of the upland forest communities of southern Wisconsin. *Ecological Monographs*, **27**, 326–349.

Brookes, P.C., Chen, Y., Chen, L., Qiu, G., Yu, L. & Xu, J. 2017. Is the rate of mineralization of soil organic carbon not under microbiological control: in search of the Regulatory Gate. *Soil Biology & Biochemistry*, **112**, 127–139.

Caporaso, J.G., Kuczynski, J., Stombaugh, J., Bittinger, K., Bushman, F.D., Costello, E.K. *et al.* 2010a. QIIME allows analysis of high-throughput community sequencing data. *Nature Methods*, **7**, 335–336.

Caporaso, J.G., Bittinger, K., Bushman, F.D., DeSantis, T.Z., Andersen, G.L. & Knight, R. 2010b. PyNAST: a flexible tool for aligning sequences to a template alignment. *Bioinformatics*, **26**, 266–267.

Dai, Z., Barberan, A., Li, Y., Brookes, P.C. & Xu, J. 2017. Bacterial community composition associated with pyrogenic organic matter (biochar) varies with pyrolysis temperature and colonization environment. *mSphere*, **2**, e00085-17.

Deenik, J.L., Diarra, A., Uehara, G., Campbell, S., Sumiyoshi, Y. & Antal, M.J. 2011. Charcoal ash and volatile matter effects on soil properties and plant growth in an acid Ultisol. *Soil Science*, **176**, 336–345.

Edgar, R.C. 2013. UPARSE: highly accurate OTU sequences from microbial amplicon reads. *Nature Methods*, **10**, 996–998.

Edgar, R.C., Haas, B.J., Clemente, J.C., Quince, C. & Knight, R. 2011. UCHIME improves sensitivity and speed of chimera detection. *Bioinformatics*, **27**, 2194–2200.

Fang, Y., Singh, B., Singh, B.P. & Krull, E. 2013. Biochar carbon stability in four contrasting soils. *European Journal of Soil Science*, **65**, 60–71.

Fang, Y., Singh, B. & Singh, B.P. 2015. Effect of temperature on biochar priming effects and its stability in soils. *Soil Biology & Biochemistry*, **80**, 136–145.

Fontaine, S., Mariotti, A. & Abbadie, L. 2003. The priming effect of organic matter: a question of microbial competition? *Soil Biology & Biochemistry*, **35**, 837–843.

Hale, L., Luth, M. & Crowley, D. 2015. Biochar characteristics relate to its utility as an alternative soil inoculum carrier to peat and vermiculite. *Soil Biology & Biochemistry*, **81**, 228–235.

He, Y., Chen, C., Xu, Z., Williams, D. & Xu, J. 2009. Assessing management impacts on soil organic matter quality in subtropical Australian forests using physical and chemical fractionation as well as ^{13}C NMR spectroscopy. *Soil Biology & Biochemistry*, **41**, 640–650.

Hilscher, A., Heister, K., Siewert, C. & Knicker, H. 2009. Mineralisation and structural changes during the initial phase of microbial degradation of pyrogenic plant residues in soil. *Organic Geochemistry*, **40**, 332–342.

Ioannidou, O. & Zabaniotou, A. 2007. Agricultural residues as precursors for activated carbon production–A review. *Renewable and Sustainable Energy Reviews*, **11**, 1966–2005.

Khodadad, C.L.M., Zimmerman, A.R., Green, S.J., Uthandi, S. & Foster, J.S. 2011. Taxa-specific changes in soil microbial community composition induced by pyrogenic carbon amendments. *Soil Biology & Biochemistry*, **43**, 385–392.

Kuzyakov, Y., Friedel, J.K. & Stahr, K. 2000. Review of mechanisms and quantification of priming effects. *Soil Biology & Biochemistry*, **32**, 1485–1498.

Kuzyakov, Y., Subbotina, I., Chen, H., Bogomolova, I. & Xu, X. 2009. Black carbon decomposition and incorporation into soil microbial biomass estimated by ^{14}C labeling. *Soil Biology & Biochemistry*, **41**, 210–219.

Lehmann, J., Rillig, M.C., Thies, J., Masiello, C.A., Hockaday, W.C. & Crowley, D. 2011. Biochar effects on soil biota–A review. *Soil Biology & Biochemistry*, **43**, 1812–1836.

Li, Y., Zhang, J., Chang, S.X., Jiang, P., Zhou, G. & Fu, S. 2013. Long-term intensive management effects on soil organic carbon pools and chemical composition in Moso bamboo (*Phyllostachys pubescens*) forests in subtropical China. *Forest Ecology and Management*, **303**, 121–130.

Li, Y., Li, Y., Chang, S., Liang, X., Qin, H., Chen, J. *et al.* 2017. Linking soil fungal community structure and function to soil organic carbon chemical

composition in intensively managed subtropical bamboo forests. *Soil Biology & Biochemistry*, **107**, 19–31.

Lu, W., Ding, W., Zhang, J., Li, Y., Luo, J., Bolan, N. *et al.* 2014. Biochar suppressed the decomposition of organic carbon in a cultivated sandy loam soil: a negative priming effect. *Soil Biology & Biochemistry*, **76**, 12–21.

Luo, Y., Durenkamp, M., De Nobili, M., Lin, Q. & Brookes, P.C. 2011. Short term soil priming effects and the mineralisation of biochar following its incorporation to soils of different pH. *Soil Biology & Biochemistry*, **43**, 2304–2314.

Luo, Y., Durenkamp, M., Lin, Q., Nobili, M., Devonshire, B.J. & Brookes, P.C. 2013. The microbial colonization and mechanisms following biochar incorporation to soils. *Soil Biology & Biochemistry*, **57**, 513–523.

Luo, Y., Yu, Z., Zhang, K., Xu, J. & Brookes, P.C. 2016. The properties and functions of biochars in forest ecosystems. *Journal of Soils and Sediments*, **16**, 2005–2020.

Luo, Y., Zang, H., Yu, Z., Chen, Z., Gunina, A., Kuzyakov, Y. *et al.* 2017. Priming effects in biochar enriched soils using a three-source-partitioning approach: ^{14}C labelling and ^{13}C natural abundance. *Soil Biology & Biochemistry*, **106**, 28–35.

Maestrini, B., Herrmann, A.M., Nannipieri, P., Schmidt, M.W.I. & Abiven, S. 2014. Ryegrass-derived pyrogenic organic matter changes organic carbon and nitrogen mineralization in a temperate forest soil. *Soil Biology & Biochemistry*, **69**, 291–301.

Maestrini, B., Nannipieri, P. & Abiven, S. 2015. A meta-analysis on pyrogenic organic matter induced priming effect. *Global Change Biology Bioenergy*, **7**, 577–590.

Mitchell, P.J., Simpson, A.J., Soong, R. & Simpson, M.J. 2015. Shifts in microbial community and water-extractable organic matter composition with biochar amendment in a temperate forest soil. *Soil Biology & Biochemistry*, **81**, 244–254.

Moral, R., Moreno-Caselles, J., Perez-Murcia, M.D., Perez-Espinosa, A., Rufete, B. & Paredes, C. 2005. Characterisation of the organic matter pool in manures. *Bioresource Technology*, **96**, 153–158.

Pezzolla, D., Marconi, G., Turchetti, B., Zadra, C., Agnelli, A., Veronesi, F. *et al.* 2015. Influence of exogenous organic matter on prokaryotic and eukaryotic microbiota in an agricultural soil. A multidisciplinary approach. *Soil Biology & Biochemistry*, **82**, 9–20.

Rousk, J., Dempster, D.N. & Jones, D.L. 2013. Transient biochar effects on decomposer microbial growth rates: evidence from two agricultural case-studies. *European Journal of Soil Science*, **64**, 770–776.

Singh, B.P. & Cowie, A.L. 2014. Long-term influence of biochar on native organic carbon mineralisation in a low-carbon clayey soil. *Scientific Reports*, **4**, 3687.

Singh, B., Singh, B.P. & Cowie, A.L. 2010. Characterisation and evaluation of biochars for their application as a soil amendment. *Australian Journal of Soil Research*, **48**, 516–525.

Singh, B.P., Cowie, A.L. & Smernik, R.J. 2012. Biochar carbon stability in a clayey soil as a function of feedstock and pyrolysis temperature. *Environmental Science & Technology*, **46**, 11770–11778.

Sohi, S.P. 2012. Carbon storage with benefits. *Science*, **338**, 1034–1035.

Tian, J., Wang, J.Y., Dippold, M., Gao, Y., Blagodatskaya, E. & Kuzyakov, Y. 2016. Biochar affects soil organic matter cycling and microbial functions but does not alter microbial community structure in a paddy soil. *Science of the Total Environment*, **556**, 89–97.

USDA 1998. *Keys for Soil Taxonomy*, 8th edn. Soil Conservation Service, Pocahontas Press, Blacksburg, VA.

Vance, E.D., Brookes, P.C. & Jenkinson, D.S. 1987. An extraction method for measuring soil microbial biomass C. *Soil Biology & Biochemistry*, **19**, 703–707.

Wardle, D.A., Nilsson, M.C. & Zackrisson, O. 2008. Fire-derived charcoal causes loss of forest humus. *Science*, **320**, 629.

Webster, R. 2007. Analysis of variance, inference, multiple comparisons and sampling effects in soil research. *European Journal of Soil Science*, **58**, 74–82.

Whitman, T., Zhu, Z.H. & Lehmann, J. 2014. Carbon mineralizability determines interactive effects on mineralization of pyrogenic organic matter and soil organic carbon. *Environmental Science & Technology*, **48**, 13727–13734.

Yuan, J.H., Xu, R.K. & Zhang, H. 2011. The forms of alkalis in the biochar produced from crop residues at different temperatures. *Bioresource Technology*, **102**, 3488–3497.